Title: Homeostatic remodeling of mammalian membranes in response to dietary lipids is essential for cellular fitness

Short title: Homeostasis of mammalian membranes

Authors: Kandice R Levental, Eric Malmberg, Robert Ernst, Ilya Levental

Authors affiliations: Kandice R Levental[a], Eric Malmberg[a], Robert Ernst[b], Ilya Levental[a]

[a]University of Texas Health Science Center at Houston, Houston, TX, USA

[b]Department of Medical Biochemistry and Molecular Biology, Medical Faculty, Saarland University, 66421 Homburg, Germany

Corresponding author: Dr. Ilya Levental

Address: Suite 4.202A, 6431 Fannin St, Houston, TX, USA 77030

Phone: +1–713–500–5566

Fax: +1–713–500–7456

Email: ilya.levental@uth.tmc.edu

Keywords: membrane fluidity, lipidomics, diet, homeostasis, adaptation, saturated lipid, polyunsaturated fatty acid, cholesterol, SREBP

Abstract: A major fraction of cellular bioactivity occurs at membranes, with the lipidic matrix constituting a functional, dynamic interface that regulates protein activity and cell physiology. Proper membrane functionality requires maintenance of a narrow range of physical properties, which must be buffered from external perturbations. The most prominent example of such maintenance is homeostatic adaptation of membrane viscosity to temperature variation, a fundamental and ubiquitous design feature of ectothermic organisms. However, such responsive membrane adaptation has not been directly observed in mammalian cells. Here, we report that challenging membrane homeostasis in mammalian cells by dietary lipids leads to robust lipidomic remodeling to preserve membrane physical properties. Specifically, exogenous polyunsaturated fatty acids (PUFAs) are rapidly and extensively incorporated into membrane lipids, inducing a reduction in membrane packing. These effects are rapidly compensated by upregulation of saturated lipids and cholesterol via activation of classical mammalian sterol regulatory machinery, which results in recovery of membrane packing. Inhibition of this compensatory response results in decreased cellular fitness when membrane homeostasis is challenged by dietary lipids. These results reveal an essential mammalian mechanism for membrane homeostasis - analogous to homeoviscous adaptation - wherein cells remodel their lipidomes in response to dietary lipid inputs in order to preserve functional membrane phenotypes.

ABSTRACT

A major fraction of cellular bioactivity occurs at membranes, with the lipidic matrix constituting a functional, dynamic interface that regulates protein activity and cell physiology. Proper membrane functionality requires maintenance of a narrow range of physical properties, which must be buffered from external perturbations. The most prominent example of such maintenance is homeostatic adaptation of membrane viscosity to temperature variation, a fundamental and ubiquitous design feature of ectothermic organisms. However, such responsive membrane adaptation has not been directly observed in mammalian cells. Here, we report that challenging membrane homeostasis in mammalian cells by dietary lipids leads to robust lipidomic remodeling to preserve membrane physical properties. Specifically, exogenous polyunsaturated fatty acids (PUFAs) are rapidly and extensively incorporated into membrane lipids, inducing a reduction in membrane packing. These effects are rapidly compensated by upregulation of saturated lipids and cholesterol via activation of classical mammalian sterol regulatory machinery, which results in recovery of membrane packing. Inhibition of this compensatory response results in decreased cellular fitness when membrane homeostasis is challenged by dietary lipids. These results reveal an essential mammalian mechanism for membrane homeostasis - analogous to homeoviscous adaptation - wherein cells remodel their lipidomes in response to dietary lipid inputs in order to preserve functional membrane phenotypes.

INTRODUCTION

Lipidic membranes are the essential barriers between life and the abiotic world and also mediate most intracellular compartmentalization in eukaryotic cells. However, the role of membranes is not limited to passive barriers. Approximately one third of all proteins are membrane-embedded [1], and many more are membrane-associated through post-translational modifications, lipid binding, and protein-protein interactions. Thus, a major fraction of cellular bioactivity occurs at or near membrane interfaces. Importantly, the physicochemical properties of the membrane matrix are key contributors to physiology. A fundamental example is membrane viscosity, which determines protein diffusivity, and thus protein-protein collision/interaction frequency. Another is membrane permeability which governs the diffusion of solutes between the cytosol and the external environment. In addition to these examples, numerous other membrane physical parameters can determine protein behavior, including but not limited to membrane fluidity, permeability, curvature, tension, packing, bilayer thickness, and lateral organization [2-12].

Because of their central role in protein function, the proper maintenance of membrane properties is essential for survival in a complex and variable environment. In ectothermic (i.e. non-thermoregulating) organisms, a pervasive challenge to membrane homeostasis comes in the form of temperature variations. Low temperature

reduces the motion of lipid acyl chains, causing membranes to laterally contract, stiffen, and become more viscous [13]. Organisms across the tree of life, from prokaryotes to ectothermic animals, respond to such perturbations by tuning membrane lipid composition, down-regulating tightly packing lipids (e.g. containing saturated acyl chains) and up-regulating more loosely packed ones containing unsaturations or methylations in their lipid tails [13-15]. This response was termed 'homeoviscous adaptation', as these lipid changes result in remarkable constancy in membrane viscosity in spite of variable growth conditions [13,14,16]. It should be noted that while viscosity is maintained, it must not be assumed that it is either the control variable, or the physical property being sensed; rather viscosity could correlate with other membrane/lipid control parameters. For example, membrane homeostasis in Bacillus subtilis is mediated by the DesK sensor that is thought to respond to membrane thickness [17]. In the yeast endoplasmic reticulum (ER), recently discovered sensors are sensitive specifically to lipid packing [5] and bilayer compressibility [18]. These key insights are exceptions to the rule, as there remains remarkably little known about the molecular mechanisms underlying the sensing of cellular membranes [15,16].

Besides a few specialized instances (e.g. hibernation), mammals and other warm-blooded animals are not subject to large-scale variations in body temperature; thus, there has been relatively little investigation of homeostatic membrane responsiveness in such organisms. However, it is a well-established but under-appreciated fact that mammalian membrane homeostasis is challenged by dietary inputs. Dietary cholesterol and fatty acids have major impacts on membrane compositions *in vivo* [19,20], and these perturbations must presumably be buffered by cellular mechanisms to maintain functionality. Mammalian lipidomes are much more complex [21-23] than either bacteria [24] or yeast [25,26], suggesting many more potential control mechanisms; however, the physiological purpose of mammalian lipidomic complexity remains opaque.

The possibility of a mammalian homeoviscous response was hypothesized from a set of studies in the 1970s, which used a spontaneously arising mutant of Chinese Hamster Ovary (CHO) cells that is defective in cholesterol regulation [27,28]. These mutants accumulate cholesterol compared to wild-type CHO cells, but maintain normal membrane fluidity, possibly through modulation of their phospholipid profiles. However, the molecular etiology of the defects in these mutants remains unknown, and it was not reported where the cholesterol in these cells was accumulating (possibly membranes, but also storage organelles or lysosomes). Further, limitations of then-available technologies prevented direct demonstration of lipidomic responses to cholesterol modulation. Thus, the relevance of those insights to physiologically relevant perturbations of metabolically normal mammalian cells remains unclear. More recently, homeoviscous adaptation in mammals has been inferred from data-driven modeling approaches, which used the physical properties (melting temperature, intrinsic curvature) of pure lipids to extrapolate those of complex, biological membranes [29,30]. However, the inherent non-additivity [31] and non-ideality [32] of lipid mixtures suggests that extrapolation of physical parameters of complex membranes from pure

99 lipids may not be a reliable approach. Finally, lipid composition and membrane properties have been implicated
100 in the heat shock response, though usually with a specific focus on signaling in the proteostasis network [33].

101 Here, we directly evaluate the homeoviscous adaptation hypothesis for mammalian membranes by characterizing
102 the consequences of membrane perturbations by dietary fatty acids in several mammalian cell types. We show
103 that polyunsaturated fatty acids (PUFAs) are specifically and robustly incorporated into membrane phospholipids,
104 introducing significant biophysical perturbations. Mammalian cells respond to this perturbation by nearly
105 concomitant lipidomic remodeling, most notably upregulation of saturated lipids and cholesterol, yielding
106 normalization of membrane biophysical properties. This response is centrally mediated by transcriptional sterol-
107 regulatory machinery involving SREBP2. Finally, we show that the homeostatic membrane response is essential
108 for cellular fitness, as abrogation of key response nodes leads to cytostatic effects when membrane homeostasis is
109 challenged by exogenous fatty acids.

110

111 **RESULTS**

112 *Specific and robust incorporation of PUFAs into membrane lipids*

113 Recent observations revealed that docosahexaenoic acid (DHA) supplementation of cultured mammalian mast
114 cells leads to robust incorporation of this dietary polyunsaturated fatty acid into membrane lipids [23]. We observed
115 similar effects in isolated human Mesenchymal Stem Cells [34], cultured Chinese hamster ovary (CHO) cells, and
116 rat primary hippocampal neurons (Supp Fig S1), suggesting that uptake and incorporation of exogenous DHA into
117 membrane lipids is not cell-type specific. To further characterize the effect, we investigated the extent,
118 destination, and time-course of exogenous FA incorporation into membrane lipids of a model mammalian cell
119 type. In rat basophilic leukemia cells (RBL), the fraction of DHA-containing glycerophospholipids (GPLs)
120 increased by nearly 15-fold (from <1 to ~15 mol%) upon supplementation of cell culture media with 20 μM DHA
121 (Fig 1A). The supplementation parameters (concentration and delivery vehicle) were selected to recapitulate
122 physiologically relevant conditions observed *in vivo* under DHA-enriched diets in mammals: ω-3 DHA
123 comprises up to 10 mol% of plasma fatty acids in rats fed a fish oil-rich diet [35], in which overall plasma free FA
124 concentrations range from 300 to 750 μM [35,36], suggesting that tens of μM are physiologically appropriate.
125 Further, ω-3 PUFA-rich diets lead to significant incorporation of these fats into cell membrane lipids *in vivo*
126 [19,35,37], with DHA-containing lipids reaching levels similar to those observed under our culture supplementation
127 conditions (Fig. 1A)[23]. Serum-containing, rather than serum-free, media was used to approximate physiological
128 supplementation, rather than exclusive introduction of specific FAs.

129 Similar to DHA, supplementation with the more common PUFA ω-6 arachidonic acid (AA) increased the fraction
130 of AA-containing lipids by >3-fold (Fig 1B). Surprisingly, supplementation with monounsaturated (oleic; OA)

acid or saturated (palmitic; PA) fatty acid produced only minimal lipidomic changes (Fig 1C-D). We speculate that this disparity in incorporation between PUFAs and more saturated FAs is associated with their availability in cell culture media. That is, cells have access to sufficient levels of OA and PA such that supplementation has no effect, whereas PUFA levels are limited such that supplementation with the physiologically appropriate concentrations used here leads to robust uptake and incorporation.

The detailed lipidomics data provided by MS/MS reveals the destination of the incorporated PUFAs. For DHA, there was notable channeling into phosphatidylethanolamine (PE) headgroup lipids, particularly those with an ether-linked hydrophobic tail (PE-O; plasmalogen). In un-supplemented cells, ~70% of all DHA was associated with a PE headgroup, despite PE lipids comprising only 25% of all GPLs. Supplementation slightly reduced this effect, although PE lipids still contained the majority of DHA (Fig 1E). These trends were markedly different for AA (Fig 1F), whose distribution more closely resembled the overall GPL headgroup profile (Supp Fig S2). Somewhat surprisingly, AA was nearly completely segregated from phosphatidylserine (PS) and phosphatidylglycerol (PG) headgroups, whereas DHA was not. These trends were also generally evident in primary human mesenchymal stem cells [34].

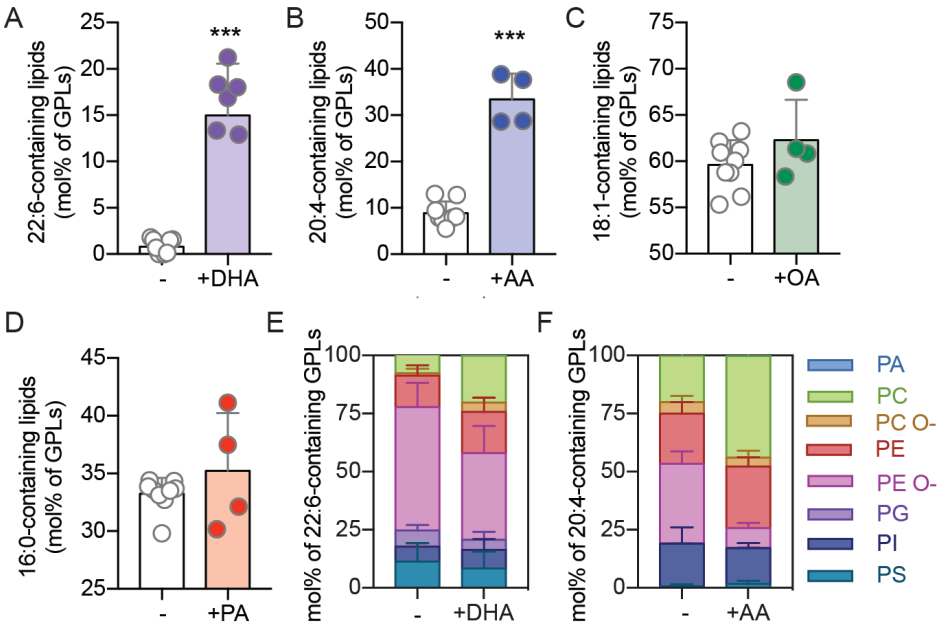

Fig 1. PUFAs are robustly and specifically incorporated into membrane phospholipids. Supplementation of culture media with (A) DHA or (B) AA for 3 days (20 μM) leads to robust enhancement of the levels of these PUFAs in membrane lipids. In contrast, supplementation with either (C) OA or (D) PA did not have observable effects on the lipidomes. (E) Before supplementation, DHA is highly non-randomly distributed among membrane phospholipids, enriching in PE-headgroup classes, most notably PE plasmalogen. Supplementation broadened the distribution of DHA into other major GPLs, though notable PE and PE-O remained. (F) AA distribution was distributed somewhat more randomly among headgroups, though with some enrichment in PI and PE. These observations reveal a notably precise targeting of w-3 PUFAs into alkyl-linked PE lipids.

153

154 *Lipidome remodeling associated with PUFA incorporation*

155 A surprising finding from these experiments was that despite the copious incorporation of exogenous PUFAs into
156 membrane lipids (Fig 1A-B) and the resulting increase in overall membrane unsaturation (Fig 2B), the cells did
157 not show any obvious toxicity or differences in proliferation. This observation was unexpected in light of the
158 central role of lipid unsaturation in membrane physical properties [38,39] and the critical role of those properties in
159 regulating various cellular processes [3,4,7]. Thus, we hypothesized that cells may be compensating for perturbations
160 from exogenous FAs by remodeling their lipidomes. Indeed, while treatments with OA/PA had no effect on the
161 overall cell lipidomes (Supp Fig S3; consistent with their lack of incorporation), both AA and DHA
162 supplementation led to a reduced abundance of other polyunsaturated (i.e. di- and tri-unsaturated) lipid species
163 (Fig 2C). This effect could potentially be explained by replacement of one PUFA by another. Much more
164 surprising was the highly significant increase in fully saturated lipids resulting from PUFA supplementation,
165 which was due in part to significantly increased abundance of phospholipid-incorporated saturated fatty acids (Fig
166 2D).

167 The increase in saturated lipids is particularly striking when lipids containing the supplemented FAs are removed
168 from the analysis (e.g. ω-3-containing lipids from DHA-supplemented data), as the rather extreme over-
169 abundance of those species upon supplementation suppresses the visualization of compensatory effects. This
170 analysis reveals approximately 2-fold and 4-fold more fully saturated lipids resulting from DHA and AA
171 supplementation, respectively (Fig 2E-F). These changes were associated with a significant net reduction in the
172 unsaturation index of GPLs not containing the supplemented FAs (Fig 2G-H). These effects were, at least in part,
173 transcriptionally mediated, as evidenced by mRNA levels of the major fatty acid desaturase enzymes SCD1 and
174 SCD2. As previously observed [40], both were substantially down-regulated by DHA treatment (Supp Fig S4), fully
175 consistent with more saturated and fewer polyunsaturated lipids.

176 A similar compensatory effect was observed for lipid length, i.e. the total number of carbons in lipid acyl chains.
177 Both AA (20-carbon) and DHA (22-carbon) are relatively long FAs, and thus their incorporation increased the
178 overall length of GPLs in the membranes (Supp Fig S5 A-B). However, there was also a notable increase in
179 relatively short non-DHA/AA containing lipids (Supp Fig S5 C-D). Surprisingly, the headgroup profile of GPLs
180 was not notably affected by any of the treatments (Fig 2A and Supp Fig S3A).

181 Importantly, the lipidomic remodeling in response to PUFA feeding was not limited to a single cell type. The
182 observations described so far were made using a transformed leukocyte cell line (RBL); however, very similar
183 DHA-induced lipid changes were observed in cultured CHO cells, primary rat hippocampal neurons, primary
184 human MSCs, and MSCs that were differentiated *in vitro* into osteoblasts or adipocytes (Fig. 2I). Remarkably, not

only the broad trends of the lipidomic remodeling (more saturated, less unsaturated lipids) were common between these disparate cell lineages and sources, but also the magnitude of the effects were quantitatively similar, despite drastic differences in overall lipid composition [23,34,41,42]. The similarity of the responses between freshly isolated cells, cultured primary cells, and long-term cultured cells lines derived from two different germ layers and three different organisms suggests that comprehensive lipidomic remodeling in response to exogenous PUFAs is a general phenomenon for mammalian cells.

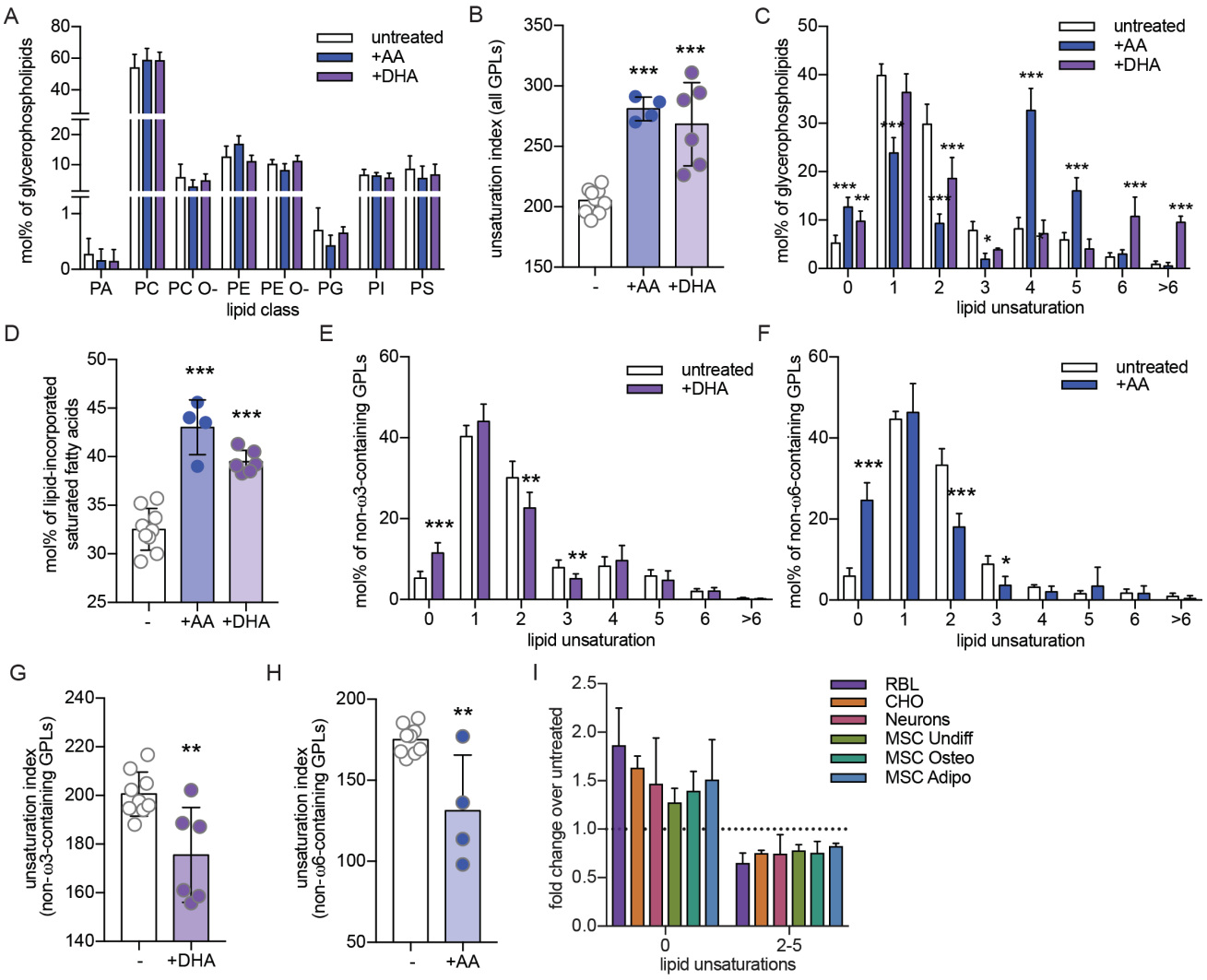

Figure 2 – Lipidome remodeling induced by PUFA supplementation. (A) Incorporation of PUFAs into membrane lipids has no effect on glycerophospholipids (GPL) headgroup distribution. (B) PUFA supplementation increases membrane unsaturated index. (C) In addition to robust incorporation of AA and DHA, fully saturated lipids are increased while other polyunsaturated lipids are reduced. (D) PUFA supplementation increased abundance of GPL-incorporated saturated fatty acids. (E-F) The compensatory effects in Fig 2C can be more clearly visualized by removing the lipid species containing the supplemented PUFAs from the analysis. (G-H) The unsaturation index of non-DHA/AA-containing lipids is significantly decreased upon PUFA supplementation. (I) DHA-mediated lipidomic remodeling, as indicated by increased saturated lipids and decreased polyunsaturated lipids (2-5 unsaturations), is consistent across multiple cell types, including isolated rat hippocampal neurons,

200 cultured human MSCs, and MSC differentiated into adipogenic or osteogenic lineages. All data shown are average +/- SD for
201 n ≥ 3 biological replicates. C, E, and F are two-way ANOVA with Sidak's multiple comparison test. B, D, G, and H are
202 student's t-test compared to untreated. *p<0.05, **p<0.01, ***p<0.001.

203

204 *Temporal characteristics of lipidomic remodeling*

205 The remodeling associated with PUFA incorporation into membrane lipids suggested the induction of a
206 homeostatic membrane response, wherein saturated lipids are upregulated to compensate for the fluidizing effect
207 of PUFA-containing species. To support this inference, we analyzed the temporal profiles of PUFA incorporation
208 and associated lipidomic changes. DHA was rapidly incorporated into membrane lipids, with significant increases
209 in DHA-containing lipids observed within 1 h of supplementation and half-time of incorporation of ~4 h (Fig 3A-
210 B). Interestingly, the recovery time course was significantly slower, as wash-out of DHA was followed by a
211 return to baseline with a half-time of ~25 h (Fig 3C). This is the approximate doubling time of RBL cells in
212 culture, suggesting that the "wash-out" effect likely results from dilution by new lipid synthesis rather than
213 directed removal of DHA from membrane lipids. Remarkably, the associated lipidome remodeling showed nearly
214 identical temporal profiles to both DHA supplementation and wash-out (Fig 3D-I). The increase in saturated
215 lipids (Fig 3E) and the decrease in di-unsaturated lipids (Fig 3H) were essentially concomitant with DHA
216 incorporation and similar time courses were also observed for the wash-out (Fig 3F and 3I). These observations
217 reveal unexpectedly rapid lipidomic changes to membrane lipid perturbations and suggest that such perturbations
218 induce nearly simultaneous compensatory responses.

219 The nature of the broad compensatory lipidomic remodeling in response to PUFA supplementation in mammalian
220 cells evokes classical observations of homeoviscous adaptation in ectothermic (e.g. non-thermoregulating)
221 organisms [13-16], wherein perturbations of membrane physical properties produced by changes in ambient
222 temperature are rapidly compensated for by lipidomic changes designed to re-normalize membrane physical
223 properties. Our findings suggest that a similar response to fluidizing stimuli occurs in mammalian cells, where it
224 has been co-opted to cope with perturbations from exogenous lipids (e.g. from the diet).

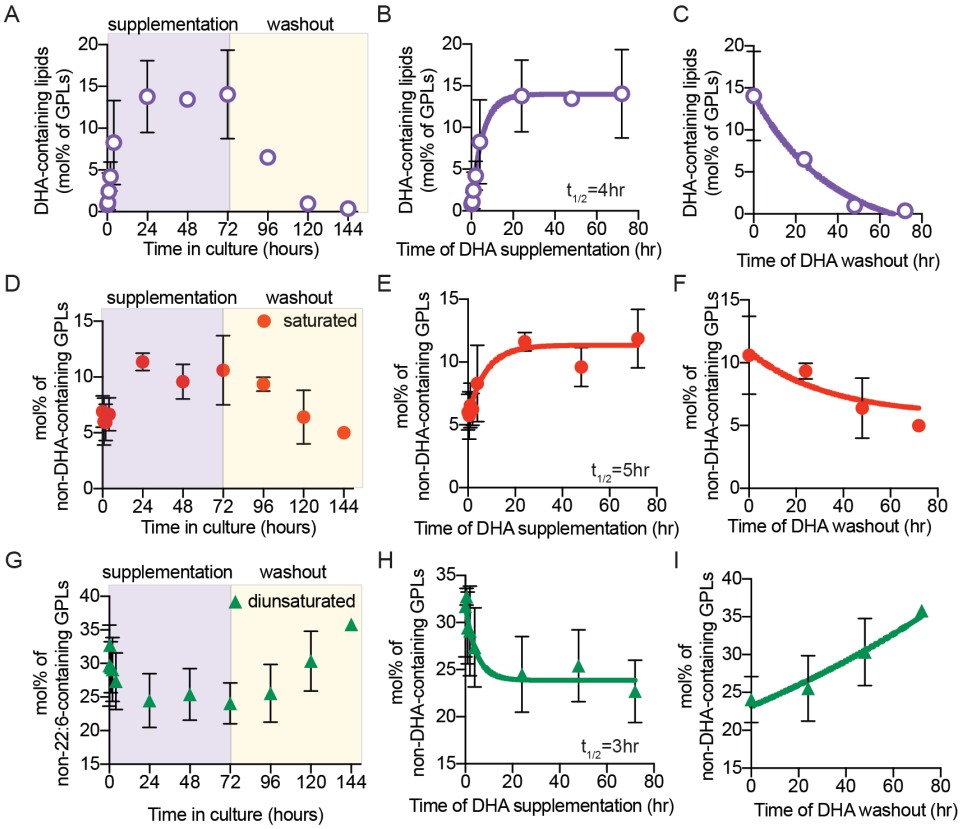

Figure 3 – Time course of DHA incorporation and lipidome remodeling. (A-C) Time course of DHA incorporation into GPLs following supplementation, then wash-out. Time course of concomitant (D-F) saturated lipid and (G-I) di-unsaturated lipid changes induced by DHA supplementation. All data shown are average +/- SD for n ≥ 3 biological replicates.

Cholesterol upregulation by DHA via SREBP2

The above-described acyl chain remodeling in response to PUFA supplementation was incomplete, as the unsaturation index of PUFA-supplemented cells remained higher than those from untreated controls (Fig 2B). If the lipidome response we observe were designed to normalize membrane properties, the acyl chain remodeling appears insufficient on its own. In contrast to most prokaryotes where membrane homeostasis is mediated almost exclusively by phospholipids [14], membrane properties in more complex organisms are regulated to a very significant extent by sterols [43,44]. Thus, we hypothesized that the adaptive response to PUFA perturbation in mammalian cells was also mediated by cholesterol. Indeed, DHA supplementation significantly increased cellular cholesterol over the un-supplemented baseline (Fig 4A). This increase in cholesterol abundance was again quite rapid, with effects observed within 1 h of DHA introduction and reaching a peak after ~4 h (Fig 4B), essentially concomitant with the acyl chain remodeling (Fig 3). There was also evidence of a small but notable overshoot, as the cholesterol increase was somewhat attenuated after ~4 hrs. These observations suggest that cholesterol upregulation is an early and potent response to membrane perturbation.

243 The machinery for cholesterol production in metazoans is regulated by proteolytic processing of transcription
244 factors of the sterol regulatory element binding protein (SREBP) family [45]. A signal to upregulate cellular
245 cholesterol level is translated into proteolysis of a membrane-bound SREBP2 precursor to release a 'mature'
246 cleaved fragment, which translocates to the nucleus to induce transcription of various target genes, including
247 those for cholesterol synthesis and uptake [45]. Having observed a robust and rapid increase in cholesterol levels
248 resulting from DHA supplementation, we evaluated whether SREBP2 processing is associated with this response.
249 Indeed, DHA feeding increased the production of the 'mature' transcription factor form of the SREBP2, with
250 minimal effects on the precursor form (Fig 4C).

251 These findings suggested that processing of SREBP2 is involved in homeostatic membrane remodeling in
252 response to perturbation of mammalian lipid composition by PUFA incorporation. To confirm this inference, we
253 measured the response to PUFA supplementation in cells lacking functional SREBP processing machinery.
254 Specifically, we used SRD-12B cells, clonal variants of CHO cells wherein a genetic defect in the Site 1 Protease
255 (S1P; cleaves SREBPs to produce the transcriptionally active forms) prevents SREBP processing/activation [46]. In
256 these cells, no notable upregulation of cholesterol (Fig 4D) or saturated lipids (Supp Fig S6) was observed upon
257 DHA supplementation, confirming the crucial role for SREBP signaling in lipidomic remodeling.

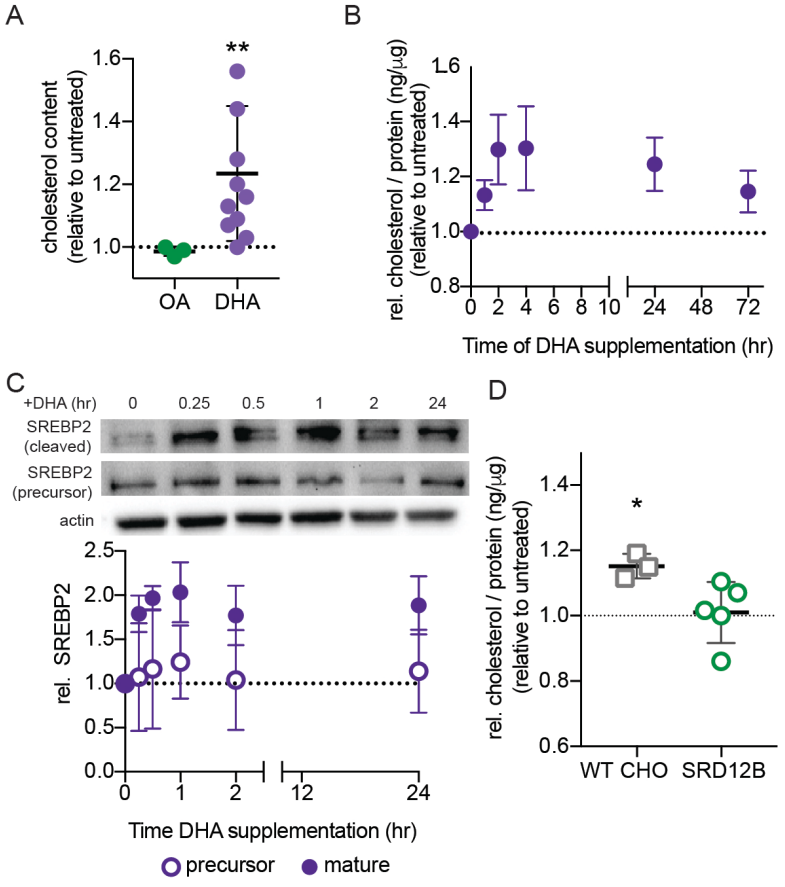

258

Fig 4 – Cholesterol upregulation by DHA supplementation. (A) Membrane cholesterol is increased by DHA supplementation. (B) Time course suggests cholesterol increase is a rapid response to DHA-mediated membrane perturbation. (C) The 'mature', transcription-competent form of SREBP2 is rapidly produced in response to DHA supplementation. (D) Cholesterol is significantly increased in WT CHO cells treated with DHA; however, in cells with abrogated SREBP activation (SRD12B; S1P-negative), there is no change in cholesterol levels with DHA supplementation. All data shown are average +/- SD for n ≥ 3 biological replicates; significances are one-sample t-test compared to untreated; *p<0.05, **p<0.01.

Order homeostasis following lipidomic perturbation

The above data reveal rapid and comprehensive lipidomic remodeling resulting from the incorporation of DHA into membrane lipids. Lipids that putatively decrease membrane fluidity / increase membrane packing (saturated lipids and cholesterol) are rapidly upregulated in response to introduction of PUFA-containing lipids that should increase membrane fluidity. These observations are consistent with lipidome remodeling for the purpose of homeostatic maintenance of membrane physical properties. To directly evaluate this inference, we measured membrane packing in live cells using a fluorescence assay that relies on a solvatochromic dye (C-Laurdan) whose spectral characteristics are dependent on membrane properties [47]. Specifically, the emission spectrum of C-Laurdan is red-shifted in loosely-packed membranes (due to the enhanced polarity of the fluorophore nano-environment), and the relative extent of this spectral shift can be quantified by ratiometric spectroscopy or imaging [48]. The resulting dimensionless parameter called Generalized Polarization (GP) is a widely used proxy for membrane packing and fluidity [49-52].

The image in Fig 5A shows a map of C-Laurdan GP in live cells generated by confocal spectral imaging [53]. This image reveals the relatively fluid (low GP; blue/green pixels) internal membranes and relatively packed plasma membranes (high GP; yellow/red pixels) characteristic of mammalian cells [48,50] (see trace right). These clearly distinct regions enabled us to separately quantify the effects of DHA on plasma versus internal membranes (Fig 5B-C). In internal membranes, we observed significantly decreased GP shortly after introduction of exogenous DHA (purple circles; pooled data for 2 and 4 h time points are different from 0 with $p < 0.01$), suggesting reduced packing consistent with the known fluidizing effect of PUFA-containing lipids [23,54]. This response eventually reversed, with fluidity returning fully to baseline at 24 h. These effects were not observed in PMs, which did not significantly diverge from baseline, and actually showed a slight trend toward increased packing with DHA (Fig 5C), possibly suggesting that PM physical properties are regulated more tightly than those of internal membranes. Thus, in both internal and PMs, DHA incorporation combined with the associated remodeling produced no net change in overall membrane properties. These microscopic observations were confirmed by spectroscopic evaluation of membrane packing in crude membrane fractions were isolated from RBL cells (Supp Fig S7).

292 Consistent with the microscopic measurements, there was no significant difference in C-Laurdan GP between
293 DHA-treated and untreated membranes after time was allowed for compensation.

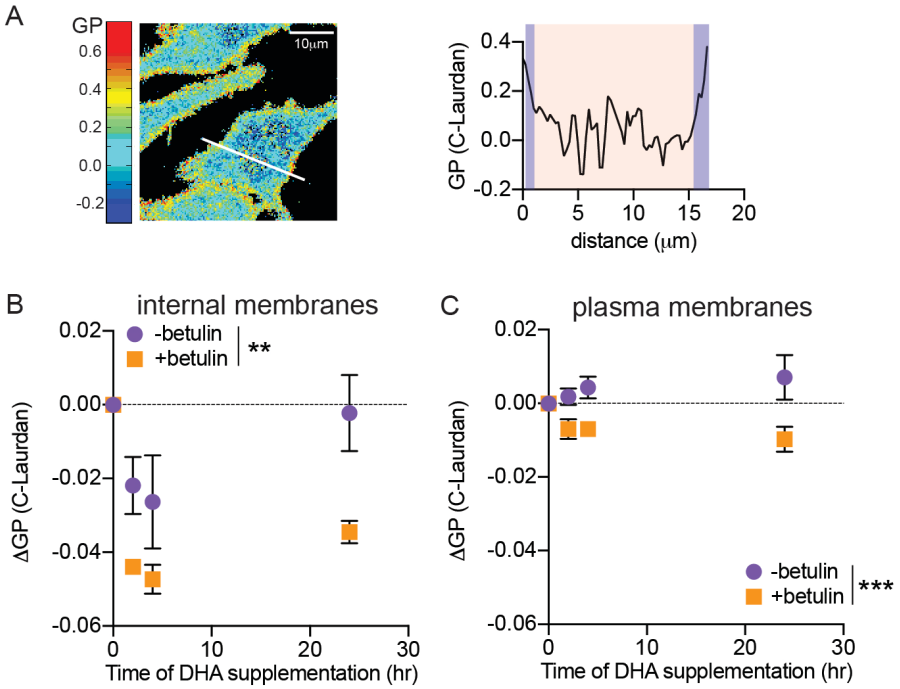

294

295 **Fig 5 – Physical membrane homeostasis.** (A) Exemplary GP map of several RBL cells showing the characteristically greater
296 GP (i.e. tighter lipid packing) of the PM compared to internal membranes. (right) The trace is a line scan of GP values across a
297 single cell shown by the white line in the image. (B) Temporal changes in lipid packing (GP) after DHA supplementation as a
298 function of betulin. In control cells, internal membranes are initially fluidized by excess DHA-containing lipids (purple), then
299 recovered to baseline by 24 hrs. In contrast, internal membrane packing did not recover in betulin-treated cells (orange). Effect
300 of treatment was highly significant ($p<0.01$) by 2-way ANOVA; each time point for betulin-treated cells was significantly
301 different from zero ($p<0.01$). (C) The effect of DHA on PMs was minimal compared to internal membranes, though betulin-
302 treated cells were significantly different from controls ($p<0.001$ by 2-way ANOVA). All data shown are average +/- SD for $n \geq 3$
303 biological replicates.

304

305 *Disruption of membrane homeostasis reduces cell fitness*

306 In unicellular organisms, the homeoviscous lipidomic response is necessary for maintaining membrane physical
307 properties in a range compatible with the biochemical processes necessary for life [13,15]. Having observed similar
308 lipidomic and biophysical responses in mammalian membranes, we hypothesized that this adaptation was
309 necessary for cellular fitness under conditions of membrane stress. To test this hypothesis, we evaluated the
310 cytostatic effects of DHA upon chemical inhibition of key nodes in the membrane response machinery,
311 specifically by inhibiting SREBP processing using the pentacyclic triterpene betulin [55]. This drug effectively
312 inhibited DHA-induced upregulation of cholesterol (Fig 6A) and saturated lipids (Supp Fig S8), and therefore

prevented the recovery of membrane packing (Fig 5B, orange squares; and Supp Fig S7), confirming the central role of SREBPs in the adaptive membrane response to DHA. More importantly, while neither DHA nor betulin alone showed significant cytostatic effects, together they led to ~50% decrease in cell number after 3 days of combined treatment (Fig 6C; full dose-response in Supp Fig S9). Similar effects were observed for inhibition of fatty acid synthase (by 10nM GSK2194069; Fig 6D), which is presumably necessary for production of fatty acids towards the phospholipid remodeling described in Figures 2-3.

These observations were confirmed in the SRD-12B cells, which have a genetic lesion that renders them incapable of activating SREBP [46]. Figs 4D and Supp Fig S6 show that these cells failed to upregulate cholesterol and saturated lipids in response to DHA. Consistently, these cells were also unable to mount an adaptive membrane response with a significant reduction in membrane packing induced by DHA (Fig 6E). Finally, while DHA slightly promoted the growth of wild-type CHO cells (Fig 6F, white), it had a marked cytostatic effect on SRD-12B cells (Fig 6F, green). These results reveal that inhibition of lipidome remodeling in mammalian cells dramatically reduced cellular fitness upon membrane perturbation with dietary fatty acids.

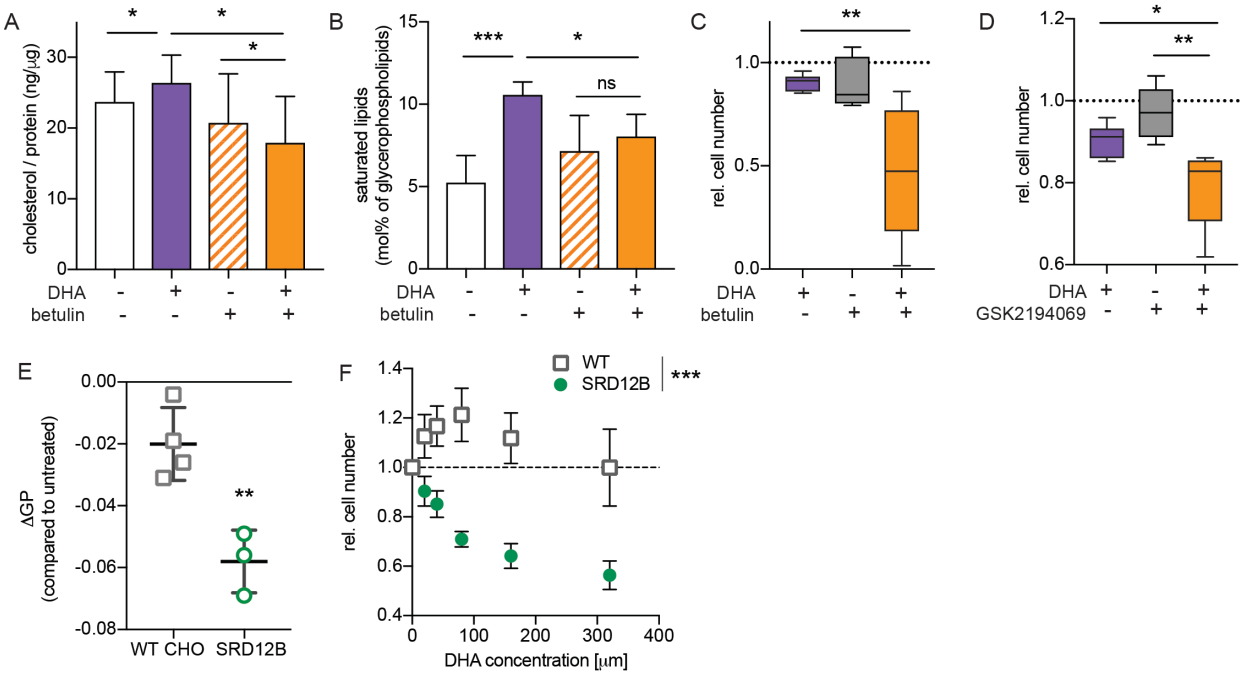

Fig 6 – Inhibition of homeostatic lipidome remodeling reduces cell fitness under DHA supplementation. (A) 200nM betulin completely abrogated DHA-induced upregulation of cholesterol and (B) saturated lipids. (C) No significant inhibition of cell number was observed by treating with either DHA or betulin (0.5 μM) alone, whereas the combination significantly reduced cell numbers. (D) A similar synergistic effect was observed with DHA and GSK2194069 (FAS inhibitor; 10 nM). (E) In SRD-12B cells, which fail to upregulate cholesterol and saturated lipids upon DHA treatment (see Fig 4D and Supp Fig S6), DHA significantly reduced membrane packing, and (F) inhibited cell growth, in contrast to control WT CHO cells, wherein DHA showed a slightly mitogenic effect. All data shown as average +/- SD for ≥3 independent experiments. A-E are student's t-tests; F is two-way ANOVA for effect of treatment. *p<0.05, **p<0.01, ***p<0.001.

335

336 **DISCUSSION**

337 The incorporation of dietary fatty acids into mammalian membrane lipids has been extensively observed both *in*
338 *vitro* [23,56,57] and *in vivo* [19,20,35,37,58]. The fact that exogenous fatty acids are so readily used for lipid synthesis is
339 unsurprising in light of the fact that the enzyme required for *de novo* fatty acid production (fatty acid synthase) is
340 expressed at minimal levels in most adult human tissues [59]. Indeed, *de novo* lipogenesis is considered "negligible"
341 [60,61] in adult humans, suggesting that exogenous sources of fatty acids are the major raw material for maintenance
342 and replenishment of membrane lipids. This reliance on exogenous inputs for production of components so
343 central to cellular architecture and function presents a major complication for mammalian membrane homeostasis.

344 In ectothermic organisms, such homeostatic membrane control has been widely observed in the form of
345 homeoviscous adaptation (HVA), which is a ubiquitous response of ectotherm cell membranes to temperature
346 variations [13-15]. According to this canonical hypothesis, the relative abundance of saturated to unsaturated
347 membrane lipids is responsive to temperatures changes in order to maintain membrane fluidity at the level
348 required for the many processes hosted and regulated by cell membranes. Although such adaptation has been
349 extensively characterized in prokaryotes [14], single-celled eukaryotes [62], and even cold-blooded animals [63,64],
350 studies on endothermic organisms have been limited [28,29], and there has yet been no direct observations of HVA in
351 mammalian cells. Our data directly confirm the three major tenets of cell-autonomous homeoviscous adaptation:
352 (1) lipidomic remodeling resulting from a perturbation of membrane physical properties (Fig 2-4); (2) recovery of
353 baseline physical properties at a new lipid composition (Fig 5); and (3) necessity of this response for cellular
354 fitness (Fig 6). These observations suggest that mammalian cells possess the capacity for homeostatic membrane
355 adaptation analogous to HVA, and that this response can be used to compensate for perturbations from dietary
356 lipid inputs.

357 In cold-blooded animals, the homeostatic membrane response also involves modulation of cholesterol levels [44,64],
358 and we observe a similar response in mammalian cells, mediated at least partially through activation of SREBP2
359 (Fig 4). It is quite remarkable to note that disruption of SREBP activation either by betulin or in SRD-12B cells
360 resulted in near-complete abrogation of the compensatory response. This abrogation was notable not only in the
361 lack of cholesterol upregulation (Fig 4D and 6A), which may have been expected, but also for upregulation of
362 saturated lipids (Figs S6 and S8), a response not obviously connected to SREBP target genes.

363 Our implication of SREBP2 as a critical node of the sense-and-respond module for membrane adaptation is fully
364 consistent with the central role of SREBPs in membrane homeostasis [45]. SREBP transcription factors have been
365 dubbed the "master regulators of lipid homeostasis", because they affect not only cholesterol synthesis and
366 uptake, but also proteins associated with membrane lipid metabolism, including those involved in FA synthesis,

367 elongation, and desaturation [65]. The effect of PUFA supplementation on SREBP function has been extensively
368 studied, and DHA is known to suppress the activation of SREBP1 and its target genes, both in cultured cells and
369 *in vivo* [66-68]. We observed downregulation of two SREBP1 target genes (SCD1 and SCD2, Supp Fig S4)
370 suggesting a similar effect in our cells. In contrast, SREBP2 is not suppressed by PUFAs [66,67], revealing that these
371 two complementary regulators of membrane homeostasis have different functions, despite both being sensitive to
372 membrane cholesterol. In our observations, SREBP2 is induced as a necessary part of the homeostatic response.
373 Previous measurements have not noted a significant effect of PUFAs on SREBP2, possibly because those
374 experiments involved acute PUFA feeding of serum-starved cells, where higher levels of activated SREBPs may
375 have suppressed the DHA-mediated stimulation we observe here. It remains to be determined whether SREBP2 is
376 simply an effector of membrane remodeling downstream of yet-unidentified sensing machinery, or whether this
377 protein (and/or its regulatory machinery) may itself be capable of sensing perturbations in membrane physical
378 properties. Direct demonstration of protein responsiveness to membrane packing has recently been described for
379 two yeast ER proteins [5,18], providing a conceptual and methodological toolbox for identifying other membrane
380 sensors. Remarkably, despite the ubiquity and importance of the homeoviscous response, the machinery used for
381 sensing membrane properties remains almost completely uncharacterized. It is an intriguing observation that Ire1,
382 a core component of the unfolded protein response (UPR), exhibits a dual sensitivity to unfolded proteins and
383 aberrant lipid compositions, demonstrating a tight connection between protein-folding and membrane properties
384 [18]. This connections suggests that the machinery for ameliorating protein-folding stresses may also be involved in
385 transducing and mitigating membrane stress [69].

386 In summary, our observations strongly support the hypothesis that mammalian cells generally possess the
387 machinery for sensing membrane physical properties and responding to perturbations by comprehensive
388 remodeling of their lipidomes. In our measurements, the major perturbations were induced by physiologically
389 relevant supplementation with polyunsaturated fatty acids (PUFAs); however, it is likely that other dietary fats
390 (e.g. cholesterol) and amphiphiles (bile acids, anesthetics) may induce similar responses. We implicate SREBP2
391 as a central response mediator, consistent with the key role of SREBPs in membrane homeostasis. Finally, we
392 show that this response is important for cell fitness, confirming membrane adaptation as a central requirement for
393 cellular homeostasis. Remarkably, detailed analysis of published fatty acid profiles of rodent[70,71] and human[58]
394 tissues suggests that fully saturated lipids are indeed upregulated *in vivo* following polyunsaturated acid feeding.
395 Although this observation was not extensively discussed in the above-referenced studies, it directly supports our
396 conclusions that mammalian cells adapt their lipidomes in response to dietary perturbations, including *in vivo*.
397

398 **MATERIALS AND METHODS**

399 ***Materials:*** Betulin and GSK2194069 were obtained from Sigma Aldrich. C-Laurdan was purchased from
400 TPProbes (South Korea). Amplex Red kit to quantify cholesterol was purchased from Invitrogen. Antibodies
401 used: actin (monoclonal clone AC-15, Abcam), SREBP2 (polyclonal, Abcam).

402 ***Cell culture:*** Rat basophilic leukemia (RBL) cells were maintained in medium containing 60% modified Eagle's
403 medium (MEM), 30% RPMI, 10% fetal calf serum, 100 units/mL penicillin, and 100 μg/mL streptomycin. CHO
404 cells were maintained in DMEM:F12 (1:1) containing 5% fetal calf serum, 100 units/mL penicillin, and 100
405 μg/mL streptomycin. SRD12B cells were maintained in DMEM:F12 (1:1) containing 5% fetal calf serum, 50μM
406 sodium mevalonate, 20μM oleic acid, 5μg/mL cholesterol, 100 units/mL penicillin, and 100 μg/mL streptomycin.
407 All cells were grown at 37°C in humidified 5% CO2.

408 ***Fatty acid treatments:*** Fatty acid stock solutions were received as air-purged ampules (Sigma Aldrich) and loaded
409 into BSA immediately upon opening. BSA loading was accompanied by stirring the fatty acid with BSA
410 dissolved in water (2:1 mol/mol FA:BSA), sterile filtering, purging with nitrogen prior to aliquoting, and storing
411 at -80°C. BSA loading, purging, and cold storage were all done to minimize FA oxidation. For all experiments
412 with FA supplementation, cells were incubated with 20 μM FA for 3 days (cells were re-supplemented 24 h prior
413 to analysis). This concentration was chosen to approximate conditions observed *in vivo* under DHA-enriched diets
414 in mammals: plasma free FA concentrations range from 300 to 750 μM [35,36] and up to 10 mol % of plasma fatty
415 acids are ω-3 DHA in rats fed a high-fish-oil diet [35]. Further, diets rich in ω-3 PUFAs led to significant
416 incorporation of these fats into cell membrane lipids [19,35,37], similar to the levels we observed under our culture
417 feeding conditions (Fig. 1). For these reasons, we believe our culture conditions reasonably approximate
418 physiological dietary membrane perturbations.

419 ***Drug treatments and cell number quantification:*** RBL cells were treated with or without 20 μM DHA in the
420 presence or absence of betulin (inhibitor of SREBP processing) or GSK2194069 (FAS inhibitor). Cells were
421 treated for 72 h and then the cell number determined via fluorescein diacetate (FDA) fluorescence. FDA is a cell
422 viability probe which freely diffuses through cell membranes, but is trapped in cells following de-acytelation by
423 cytoplasmic esterases in viable cells. The number of viable cells is then directly related to fluorescein
424 fluorescence intensity. For the assay, cells were treated in 96-well plates, gently washed with PBS, and then
425 incubated with fluorescein diacetate (5 μg/mL in PBS) for 2 minutes at 37°C. The plates were then washed again
426 to remove excess FDA and fluorescence was measured at 488 nm excitation and 520 nm emission. For each
427 experiment the number of cells per well were normalized to untreated, unsupplemented cells.

428 ***Lipidomics:*** Detailed lipidomic analysis was performed by Lipotype, GmbH, as previously described[72]. Briefly,
429 for preparation of crude cell membranes, cells were washed with phosphate buffered saline (PBS), scraped in 10
430 mM Tris pH 7.4, and then homogenized with a 27-gauge needle. Nuclei were then pelleted by centrifugation at

431 300 xg for 5 min. The supernatant was pelleted by centrifugation at 100,000 xg for 1 h at 4°C. The membrane
432 pellet was then washed and resuspended in 150 mM ammonium bicarbonate.

433 *Lipids detected*: ceramide (Cer), Chol, SM, diacylglycerol (DAG), lactosyl ceramide (DiHexCer),
434 glucosyl/galactosyl ceramide (HexCer), sterol ester (SE), and triacylglycerol (TAG), as well as phosphatidic acid
435 (PA), phosphatidylcholine (PC), phosphatidylethanolamine (PE), phosphatidylglycerol (PG), and
436 phosphatidylinositol (PI), phosphatidylserine (PS), and their respective lysospecies (lysoPA, lysoPC, lysoPE,
437 lysoPI, and lysoPS) and ether derivatives (PC O-, PE O-, LPC O-, and LPE O-). Lipid species were annotated
438 according to their molecular composition as follows: [lipid class]-[sum of carbon atoms in the FAs]:[sum of
439 double bonds in the FAs];[sum of hydroxyl groups in the long chain base and the FA moiety] (e.g., SM-32:2;1).
440 When available, the individual FA composition according to the same rule is given in brackets (e.g., 18:1;0-
441 24:2;0)

442 *Lipid extraction*: Samples were extracted and analyzed as previously described (39,47), which is a modification
443 of a previously published method for shotgun lipidomics (48). Briefly, membrane samples were suspended in 150
444 μL of 150 mM ammonium bicarbonate in water, spiked with 20 μL of internal standard lipid mixture, and then
445 extracted with 750 μL of a chloroform/methanol 10:1 (v/v) mixture for 2 h at 4_C with 1400 rpm shaking. After
446 centrifugation (3 min, 3000 **g**) to facilitate phase partitioning, the lower, lipid-containing, organic phase was
447 collected (first-step extract), and the remaining water phase was further extracted with 750 μL of a
448 chloroform/methanol 2:1 (v/v) mixture under the same conditions. Again the lower, organic phase was collected
449 (second-step extract). Extracts were dried in a speed vacuum concentrator, and 120 μL of a dried first-step extract
450 underwent acetylation with 75 μL of an acetyl chloride/chloroform 1:2 (v/v) mixture for 1 h to derivatize Chol.
451 After the reaction was completed, the mixture was dried. Then, 120 μL of a dried first-step extract and a
452 derivatized extract were resuspended in an acquisition mixture with 8 mM ammonium acetate (400 mM
453 ammonium acetate in methanol/chloroform/methanol/propan-2-ol, 1:7:14:28, v/v/v/v). Next, 120 μL of the
454 second-step extract was resuspended in an acquisition mixture with 30 μL 33% methylamine in methanol, in 60
455 mL methanol/chloroform 1:5 (v/v). All liquid-handling steps were performed using a Hamilton (Reno, NV)
456 STARlet robotic platform with the Anti Droplet Control feature, ensuring the accuracy and reproducibility of
457 organic solvent pipetting.

458 *Lipid standards*: Synthetic lipid standards were purchased from Sigma-Aldrich (Chol D6), Larodan (Solna,
459 Sweden) Fine Chemicals (DAG and TAG), and Avanti Polar Lipids (all others). The standard lipid mixtures were
460 chloroform/ methanol 1:1 (v/v) solutions containing Cer 35:1;2, (D18:1;2, 17:0;0); Chol D6; DAG 34:0;0 (17:0;0,
461 17:0;0); DiHexCer 30:1;2 (D18:1;2.12:0;0); HexCer 30:1;2 (D18:1;2.12:0;0); LPA 17:0;0 (17:0;0); LPC 12:0;0
462 (12:0;0); LPE 17:1;0 (17:1;0); LPI 17:1;0 (17:1;0); LPS 17:1;0 (17:1;0); PA 34:0;0 (17:0;0, 17:0;0); PC 34:0;0

463 (17:0;0, 17:0;0); PE 34:0;0 (17:0;0, 17:0;0); PG 34:0;0 (17:0;0, 17:0;0); PI 32:0;0 (16:0;0, 16:0;0); PS 34:0;0
464 (17:0;0, 17:0;0); SE 20:0;0 (20:0;0); SM 30:1;2 (18:1;2, 12:0;0); and TAG 51:0;0 (17:0;0, 17:0;0, 17:0;0).

465 *Lipid spectrum acquisition:* Extracts in the acquisition mixtures were infused with a robotic nanoflow ion source
466 (TriVersa NanoMate; Advion Biosciences, Ithaca, NY) into a mass spectrometer instrument (Q Exactive, Thermo
467 Scientific). Cer, DiHexCer, HexCer, lysolipids, and SM were monitored by negative ion mode Fourier transform
468 mass spectrometry (FT-MS). PA, PC, PE, PI, PS, and ether species were monitored by negative ion mode FT
469 tandem MS (FT-MS/MS). Acetylated Chol was monitored by positive ion mode FTMS. SE, DAG, TAG, and
470 species were monitored by positive ion mode FT-MS/MS.

471 *Lipid identification and quantification:* Automated processing of acquired mass spectra, and identification and
472 quantification of detected molecular lipid species were performed with the use of LipidXplorer software (17).
473 Only lipid identifications with a signal/noise ratio of >5, an absolute abundance of at least 1 pmol, and a signal
474 intensity fivefold higher than in the corresponding blank samples were considered for further data analysis.

475 ***C-laurdan spectroscopy:.*** Membrane packing (related to order and fluidity) was determined via C-laurdan
476 spectroscopy as described [73,74]. Briefly, cells were washed with PBS and stained with 20 µg/mL C-laurdan for 10
477 minutes on ice. The emission spectrum from isolated GPMVs was gathered from 400-550 nm with excitation at
478 385 nm at 23°C. The GP was calculated according to the following equation:
479

480 $$GP = \frac{\sum_{420}^{460} I_x - \sum_{470}^{510} I_x}{\sum_{420}^{460} I_x + \sum_{470}^{510} I_x}$$

481

482 ***C-Laurdan spectral imaging:*** C-Laurdan imaging was performed as previously described [23,34,53,73,74]. Briefly, cells
483 were washed with PBS and stained with 10 µg/mL C-Laurdan for 10 min on ice, then imaged via confocal
484 microscopy on a Nikon A1R with spectral imaging at 60x and excitation at 405 nm. The emission was collected
485 in two bands: 433–463 nm and 473–503 nm. MATLAB (MathWorks, Natick, MA) was used to calculate the two-
486 dimensional (2D) GP map, where GP for each pixel was calculated from a ratio of the two fluorescence channels,
487 as previously described [53]. Briefly, each image was binned (2x2), background subtracted, and thresholded to keep
488 only pixels with intensities greater than 3 standard deviations of the background value in both channels. The GP
489 image was calculated for each pixel using the above equation. GP maps (pixels represented by GP value rather
490 than intensity) were imported into ImageJ. Line scans were drawn across individual cells. PM GP values were
491 calculated as averages of the peaks as values higher than 0.26. For internal membranes, average GP values were
492 calculated from line scans around the nucleus (visible as a dark spot in C-Laurdan images). At least 10 cells were
493 imaged and quantified per experiment with at least 4 individual experiments performed. Reported are the mean
494 and standard deviations of the average GP values for the individual experiments.

495

496 ***Amplex Red assay:*** Amplex Red cholesterol assay was performed (according to manufacturer instructions;
497 Invitrogen) to determine the abundance of cholesterol. Each reading was normalized to protein concentration
498 (determined by bicinchoninic acid (BCA) assay) in the same samples. Technical triplicates were measured for
499 each sample. Shown are values normalized to untreated cells. Reported are the average and standard deviations
500 from at least 3 independent biological replicates.

501

502 ***Western Blot:*** Cells were washed with ice cold PBS, then scraped into Laemmli lysis buffer (50mM Tris-HCl, pH
503 8.0; 2% SDS; 5mM EDTA, pH8.0) supplemented with protease inhibitor cocktail. Protein concentration was
504 determined using BCA (Pierce), and equal amounts of protein were mixed with reducing Laemmli sample buffer
505 and loaded onto SDS-PAGE gels. Gels were transferred to PVDF membranes, which were blocked in 5% BSA.
506 Membranes were incubated with primary antibodies overnight at 4°C, and detected with either AlexaFluor or
507 HRP-tagged secondary antibodies. Membranes were imaged using a BioRad ChemiDoc imager. The intensities
508 of the bands were quantified normalized to actin, and plotted as mean ± SD of $n \geq 3$ experiments.

509

510 ***Real Time Quantitative PCR:*** Total RNA was isolated via Trizol (Sigma) following the manufacturer's protocol.
511 Reverse transcriptase PCR was performed using the High Capacity cDNA Reverse Transcription Kit from
512 Applied Biosystems according to manufacturer's protocol. To quantify mRNA expression, SYBR Fast MasterMix
513 (2x) Universal Dye (#KK4602) from Kapa Biosystems was used in an Eppendorf Realplex2 Mastercycler. Each
514 primer set for each sample was run in triplicate with 1 ng of cDNA per well. The primer sets used are:

515

516

Gene	**Forward Primer**	**Reverse Primer**
GAPDH	GTCTACTGGCGTCTTCACCA	GTGGCAGTGATGGCATGGAC
SCD1	GTGATGTTCCAGAGGAGGTACT	CAGGAACTCAGAAGCCCAGAA
SCD2	GGTGATGTTCCAGAGGAGGTATT	AACTGGAAGACCCCGAACTC

517

518 Expression changes were calculated using the delta delta C_T method. The data was standardized using a
519 previously published protocol [75] in which the average fold change was log transformed, mean centered, and
520 confidence intervals determined to evaluate statistical significance.

521

522 **Acknowledgements**

523 All confocal microscopy was performed at the Center for Advanced Microscopy, Department of Integrative
524 Biology and Pharmacology McGovern Medical School at the University of Texas Health Science Center at
525 Houston. We acknowledge funding from the Cancer Prevention Research Institute of Texas (CPRIT; R1215),
526 NIH/National Institute of General Medical Sciences (grant nos. GM114282, GM124072, GM120351), and the
527 Volkswagen Foundation (grant no. 93091).

528

529 **References**

530 1 Krogh, A., Larsson, B., von Heijne, G. & Sonnhammer, E. L. Predicting transmembrane protein topology
531 with a hidden Markov model: application to complete genomes. *Journal of molecular biology* **305**, 567-
532 580, (2001).
533 2 Janmey, P. A. & Kinnunen, P. K. Biophysical properties of lipids and dynamic membranes. *Trends in cell*
534 *biology* **16**, 538-546, (2006).
535 3 Los, D. A. & Murata, N. Membrane fluidity and its roles in the perception of environmental signals.
536 *Biochim Biophys Acta* **1666**, 142-157, (2004).
537 4 Andersen, O. S. & Koeppe, R. E., 2nd. Bilayer thickness and membrane protein function: an energetic
538 perspective. *Annu Rev Biophys Biomol Struct* **36**, 107-130, (2007).
539 5 Covino, R. *et al.* A Eukaryotic Sensor for Membrane Lipid Saturation. *Molecular cell* **63**, 49-59, (2016).
540 6 daCosta, C. J., Dey, L., Therien, J. P. & Baenziger, J. E. A distinct mechanism for activating uncoupled
541 nicotinic acetylcholine receptors. *Nat Chem Biol* **9**, 701-707, (2013).
542 7 Marsh, D. Protein modulation of lipids, and vice-versa, in membranes. *Biochim Biophys Acta* **1778**, 1545-
543 1575, (2008).
544 8 Roux, A. *et al.* Membrane curvature controls dynamin polymerization. *Proc Natl Acad Sci U S A* **107**,
545 4141-4146, (2010).
546 9 Shi, Z. & Baumgart, T. Membrane tension and peripheral protein density mediate membrane shape
547 transitions. *Nature communications* **6**, 5974, (2015).
548 10 Rosholm, K. R. *et al.* Membrane curvature regulates ligand-specific membrane sorting of GPCRs in
549 living cells. *Nat Chem Biol* **13**, 724-729, (2017).
550 11 Sezgin, E., Levental, I., Mayor, S. & Eggeling, C. The mystery of membrane organization: composition,
551 regulation and roles of lipid rafts. *Nat Rev Mol Cell Biol* **18**, 361-374, (2017).
552 12 Lorent, J. H. *et al.* Structural determinants and functional consequences of protein affinity for membrane
553 rafts. *Nature communications* **8**, 1219, (2017).
554 13 Hazel, J. R. Thermal adaptation in biological membranes: is homeoviscous adaptation the explanation?
555 *Annu Rev Physiol* **57**, 19-42, (1995).
556 14 Sinensky, M. Homeoviscous adaptation--a homeostatic process that regulates the viscosity of membrane
557 lipids in Escherichia coli. *Proc Natl Acad Sci U S A* **71**, 522-525, (1974).
558 15 Ernst, R., Ejsing, C. S. & Antonny, B. Homeoviscous adaptation and the regulation of membrane lipids.
559 *Journal of molecular biology* **428**, 4776-4791, (2016).
560 16 Guschina, I. A. & Harwood, J. L. Mechanisms of temperature adaptation in poikilotherms. *FEBS Lett*
561 **580**, 5477-5483, (2006).
562 17 Aguilar, P. S. *et al.* Molecular basis of thermosensing: a two-component signal transduction thermometer
563 in Bacillus subtilis. *EMBO J* **20**, 1681-1691, (2001).
564 18 Halbleib, K. *et al.* Activation of the Unfolded Protein Response by Lipid Bilayer Stress. *Molecular cell*
565 **67**, 673-684 e678, (2017).
566 19 Cao, J., Schwichtenberg, K. A., Hanson, N. Q. & Tsai, M. Y. Incorporation and clearance of omega-3
567 fatty acids in erythrocyte membranes and plasma phospholipids. *Clinical chemistry* **52**, 2265-2272,
568 (2006).

569 20 Oliveira, T. V. *et al.* Impact of high cholesterol intake on tissue cholesterol content and lipid transfers to
570 high-density lipoprotein. *Nutrition* **27**, 713-718, (2011).
571 21 Gerl, M. J. *et al.* Quantitative analysis of the lipidomes of the influenza virus envelope and MDCK cell
572 apical membrane. *J Cell Biol* **196**, 213-221, (2012).
573 22 Sampaio, J. L. *et al.* Membrane lipidome of an epithelial cell line. *Proc Natl Acad Sci U S A* **108**, 1903-
574 1907, (2011).
575 23 Levental, K. R. *et al.* Polyunsaturated lipids regulate membrane domain stability by tuning membrane
576 order. *Biophys J* **110(8)**, 1800-1810, (2016).
577 24 Han, X. in *Lipidomics* 427-442 (John Wiley & Sons, Inc, 2016).
578 25 Klemm, R. W. *et al.* Segregation of sphingolipids and sterols during formation of secretory vesicles at the
579 trans-Golgi network. *J Cell Biol* **185**, 601-612, (2009).
580 26 Ejsing, C. S. *et al.* Global analysis of the yeast lipidome by quantitative shotgun mass spectrometry. *Proc*
581 *Natl Acad Sci U S A* **106**, 2136-2141, (2009).
582 27 Sinensky, M. Defective regulation of cholesterol biosynthesis and plasma membrane fluidity in a Chinese
583 hamster ovary cell mutant. *Proc Natl Acad Sci U S A* **75**, 1247-1249, (1978).
584 28 Sinensky, M. Adaptive alteration in phospholipid composition of plasma membranes from a somatic cell
585 mutant defective in the regulation of cholesterol biosynthesis. *J Cell Biol* **85**, 166-169, (1980).
586 29 Dymond, M. K. Mammalian phospholipid homeostasis: homeoviscous adaptation deconstructed by
587 lipidomic data driven modelling. *Chem Phys Lipids* **191**, 136-146, (2015).
588 30 Dymond, M. K., Hague, C. V., Postle, A. D. & Attard, G. S. An in vivo ratio control mechanism for
589 phospholipid homeostasis: evidence from lipidomic studies. *J R Soc Interface* **10**, 20120854, (2013).
590 31 Sodt, A. J., Venable, R. M., Lyman, E. & Pastor, R. W. Nonadditive Compositional Curvature Energetics
591 of Lipid Bilayers. *Phys Rev Lett* **117**, 138104, (2016).
592 32 Almeida, P. F. Thermodynamics of lipid interactions in complex bilayers. *Biochim Biophys Acta* **1788**,
593 72-85, (2009).
594 33 Balogh, G. *et al.* Key role of lipids in heat stress management. *FEBS Lett* **587**, 1970-1980, (2013).
595 34 Levental, K. R. *et al.* omega-3 polyunsaturated fatty acids direct differentiation of the membrane
596 phenotype in mesenchymal stem cells to potentiate osteogenesis. *Science advances* **3**, eaao1193, (2017).
597 35 Yaqoob, P. *et al.* Comparison of the effects of a range of dietary lipids upon serum and tissue lipid
598 composition in the rat. *The international journal of biochemistry & cell biology* **27**, 297-310, (1995).
599 36 Pirro, M. *et al.* Plasma free fatty acid levels and the risk of ischemic heart disease in men: prospective
600 results from the Quebec Cardiovascular Study. *Atherosclerosis* **160**, 377-384, (2002).
601 37 Metcalf, R. G. *et al.* Effects of fish-oil supplementation on myocardial fatty acids in humans. *The*
602 *American journal of clinical nutrition* **85**, 1222-1228, (2007).
603 38 van Blitterswijk, W. J., van der Meer, B. W. & Hilkmann, H. Quantitative contributions of cholesterol
604 and the individual classes of phospholipids and their degree of fatty acyl (un)saturation to membrane
605 fluidity measured by fluorescence polarization. *Biochemistry* **26**, 1746-1756, (1987).
606 39 Lande, M. B., Donovan, J. M. & Zeidel, M. L. The relationship between membrane fluidity and
607 permeabilities to water, solutes, ammonia, and protons. *J Gen Physiol* **106**, 67-84, (1995).
608 40 Sessler, A. M., Kaur, N., Palta, J. P. & Ntambi, J. M. Regulation of stearoyl-CoA desaturase 1 mRNA
609 stability by polyunsaturated fatty acids in 3T3-L1 adipocytes. *J Biol Chem* **271**, 29854-29858, (1996).
610 41 Levental, I. & Veatch, S. L. The continuing mystery of lipid rafts. *J. Mol. Biol.* **428**, 4749-4764, (2016).
611 42 Lin, X. *et al.* Domain Stability in Biomimetic Membranes Driven by Lipid Polyunsaturation. *J Phys*
612 *Chem B* **120**, 11930-11941, (2016).
613 43 Yeagle, P. L. Cholesterol and the cell membrane. *Biochim Biophys Acta* **822**, 267-287, (1985).
614 44 Crockett, E. Cholesterol Function in Plasma Membranes from Ectotherms: Membrane-Specific Roles in
615 Adaptation to Temperature. *Integrative and Comparative Biology* **38**, 298-304, (1998).
616 45 Raghow, R. *et al.* SREBPs: the crossroads of physiological and pathological lipid homeostasis. *Trends*
617 *Endocrinol Metab* **19**, 65-73, (2008).
618 46 Sakai, J. *et al.* Molecular identification of the sterol-regulated luminal protease that cleaves SREBPs and
619 controls lipid composition of animal cells. *Molecular cell* **2**, 505-514, (1998).

620 47 Kim, H. M. *et al.* A two-photon fluorescent probe for lipid raft imaging: C-laurdan. *Chembiochem* **8**, 553-
621 559, (2007).
622 48 Owen, D. M. *et al.* Quantitative imaging of membrane lipid order in cells and organisms. *Nat Protoc* **7**,
623 24-35, (2011).
624 49 Kaiser, H. J. *et al.* Order of lipid phases in model and plasma membranes. *Proc Natl Acad Sci U S A* **106**,
625 16645-16650, (2009).
626 50 Gaus, K. *et al.* Condensation of the plasma membrane at the site of T lymphocyte activation. *J Cell Biol*
627 **171**, 121-131, (2005).
628 51 Parasassi, T. *et al.* Quantitation of lipid phases in phospholipid vesicles by the generalized polarization of
629 Laurdan fluorescence. *Biophys J* **60**, 179-189, (1991).
630 52 Sezgin, E. *et al.* Adaptive lipid packing and bioactivity in membrane domains. *PloS one* **10**, e0123930,
631 (2015).
632 53 Sezgin, E., Waithe, D., Bernardino de la Serna, J. & Eggeling, C. Spectral imaging to measure
633 heterogeneity in membrane lipid packing. *Chemphyschem* **16**, 1387-1394, (2015).
634 54 Feller, S. E., Gawrisch, K. & MacKerell, A. D., Jr. Polyunsaturated fatty acids in lipid bilayers: intrinsic
635 and environmental contributions to their unique physical properties. *J Am Chem Soc* **124**, 318-326,
636 (2002).
637 55 Tang, J. J. *et al.* Inhibition of SREBP by a small molecule, betulin, improves hyperlipidemia and insulin
638 resistance and reduces atherosclerotic plaques. *Cell Metab* **13**, 44-56, (2011).
639 56 Briolay, A., Jaafar, R., Nemoz, G. & Bessueille, L. Myogenic differentiation and lipid-raft composition of
640 L6 skeletal muscle cells are modulated by PUFAs. *Biochim Biophys Acta* **1828**, 602-613, (2013).
641 57 Seo, J. *et al.* Docosahexaenoic acid selectively inhibits plasma membrane targeting of lipidated proteins.
642 *FASEB journal : official publication of the Federation of American Societies for Experimental Biology*
643 **20**, 770-772, (2006).
644 58 Stark, K. D. *et al.* Fatty acid compositions of serum phospholipids of postmenopausal women: a
645 comparison between Greenland Inuit and Canadians before and after supplementation with fish oil.
646 *Nutrition* **18**, 627-630, (2002).
647 59 Kusakabe, T. *et al.* Fatty acid synthase is expressed mainly in adult hormone-sensitive cells or cells with
648 high lipid metabolism and in proliferating fetal cells. *J Histochem Cytochem* **48**, 613-622, (2000).
649 60 Weiss, L. *et al.* Fatty-acid biosynthesis in man, a pathway of minor importance. Purification, optimal
650 assay conditions, and organ distribution of fatty-acid synthase. *Biol Chem Hoppe Seyler* **367**, 905-912,
651 (1986).
652 61 Murphy, E. J. Stable isotope methods for the in vivo measurement of lipogenesis and triglyceride
653 metabolism. *J Anim Sci* **84 Suppl**, E94-104, (2006).
654 62 Nakagawa, Y., Sakumoto, N., Kaneko, Y. & Harashima, S. Mga2p is a putative sensor for low
655 temperature and oxygen to induce OLE1 transcription in Saccharomyces cerevisiae. *Biochem Biophys Res*
656 *Commun* **291**, 707-713, (2002).
657 63 Tiku, P. E. *et al.* Cold-induced expression of delta 9-desaturase in carp by transcriptional and
658 posttranslational mechanisms. *Science* **271**, 815-818, (1996).
659 64 Burns, M. *et al.* Miscibility Transition Temperature Scales with Growth Temperature in a Zebrafish Cell
660 Line. *Biophys J* **113**, 1212-1222, (2017).
661 65 Eberle, D. *et al.* SREBP transcription factors: master regulators of lipid homeostasis. *Biochimie* **86**, 839-
662 848, (2004).
663 66 Yahagi, N. *et al.* A crucial role of sterol regulatory element-binding protein-1 in the regulation of
664 lipogenic gene expression by polyunsaturated fatty acids. *J Biol Chem* **274**, 35840-35844, (1999).
665 67 Hannah, V. C. *et al.* Unsaturated fatty acids down-regulate srebp isoforms 1a and 1c by two mechanisms
666 in HEK-293 cells. *J Biol Chem* **276**, 4365-4372, (2001).
667 68 Xu, J. *et al.* Polyunsaturated fatty acids suppress hepatic sterol regulatory element-binding protein-1
668 expression by accelerating transcript decay. *J Biol Chem* **276**, 9800-9807, (2001).

69 Radanovic, T. *et al.* An Emerging Group of Membrane Property Sensors Controls the Physical State of Organellar Membranes to Maintain Their Identity. *BioEssays : news and reviews in molecular, cellular and developmental biology*, e1700250, (2018).
70 Fan, Y. Y., McMurray, D. N., Ly, L. H. & Chapkin, R. S. Dietary (n-3) polyunsaturated fatty acids remodel mouse T-cell lipid rafts. *The Journal of nutrition* **133**, 1913-1920, (2003).
71 Fan, Y. Y. *et al.* Dietary docosahexaenoic acid suppresses T cell protein kinase C theta lipid raft recruitment and IL-2 production. *J Immunol* **173**, 6151-6160, (2004).
72 Tulodziecka, K. *et al.* Remodeling of the postsynaptic plasma membrane during neural development. *Mol Biol Cell* **27**, 3480-3489, (2016).
73 Sezgin, E. *et al.* Elucidating membrane structure and protein behavior using giant plasma membrane vesicles. *Nat Protoc* **7**, 1042-1051, (2012).
74 Levental, K. R. & Levental, I. Isolation of giant plasma membrane vesicles for evaluation of plasma membrane structure and protein partitioning. *Methods in molecular biology* **1232**, 65-77, (2015).
75 Willems, E., Leyns, L. & Vandesompele, J. Standardization of real-time PCR gene expression data from independent biological replicates. *Analytical biochemistry* **379**, 127-129, (2008).